SUMMARY OF THE 2014 BEAM-HALO MONITORING WORKSHOP*

Alan S. Fisher[#], SLAC National Accelerator Laboratory, Menlo Park, California 94025, USA

Abstract

Understanding and controlling beam halo is important for high-intensity hadron accelerators, for high-brightness electron linacs, and for low-emittance light sources. This can only be achieved by developing suitable diagnostics. The main challenge faced by such instrumentation is the high dynamic range needed to observe the halo in the presence of an intense core. In addition, measurements must often be made non-invasively.

This talk summarizes the one-day workshop on Beam-Halo Monitoring that was held at SLAC on September 19 last year, immediately following IBIC 2014 in Monterey. Workshop presentations described invasive techniques using wires, screens, or crystal collimators, and non-invasive measurements with gas or scattered electrons. Talks on optical methods showed the close links between observing halo and astronomical problems like observing the solar corona or directly observing a planet orbiting another star.

INTRODUCTION

There were 39 participants [1] in the workshop on beam-halo monitoring [2]. This paper summarizes the 11 talks and draws from the slides, which are posted on-line [3], without additional reference numbers. Each contributor's name appears in **boldface** when first cited below, and appears again in figure captions.

The subject of beam halo was introduced by **Kay Wittenburg** (DESY). Although a broad definition is difficult, "halo is low density and therefore difficult to measure." Charge near the core of a bunched beam, with a density of 10^{-1} to 10^{-4} of the peak, is commonly considered a "tail". Halo has even lower densities and is often further from the core, although there are no clear boundaries (Figure 1). The dynamic range required for measurement can span 5 to perhaps 8 orders of magnitude, depending on the number of poorly bunched, high-energy particles needed to damage the machine.

Halo has a variety of sources, including space-charge or beam-beam forces; poorly matched, misaligned or non-linear accelerator optics; instabilities and resonances; RF noise; scattering (intra-beam, residual gas, macroparticles, photons, obstacles, stripping foil, screens, etc.); electron clouds; beam-energy tails from uncaptured particles; or transverse-longitudinal coupling in the RF field.

Quantifying halo is made more difficult by varying definitions. Also, oscillations in phase space may cause measurements using projections into real space to vary with position along the machine. The techniques fall into three broad groupings: invasive measurements (wire
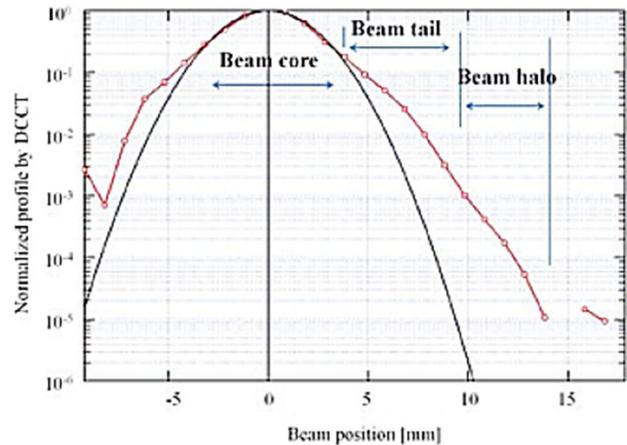

Figure 1: A beam profile showing core, tail, and halo (log scale). (K. Wittenburg, from M. Yoshimoto [4])

scanners, scrapers); non-invasive, non-optical methods (gas jets, electrons); and optical measurements. Workshop talks presented many of these approaches.

INVASIVE TECHNIQUES

Wire Scanners

Pavel Evtushenko (Jefferson Lab) stressed the need to protect electron linacs with continuous RF and MW beams from damage due to beam loss from tails and halos. Even in idealized Parmela simulations, the JLab FEL injector forms a tail at the level of 3×10^{-3}. Images using optical transition radiation (OTR) and YAG:Ce
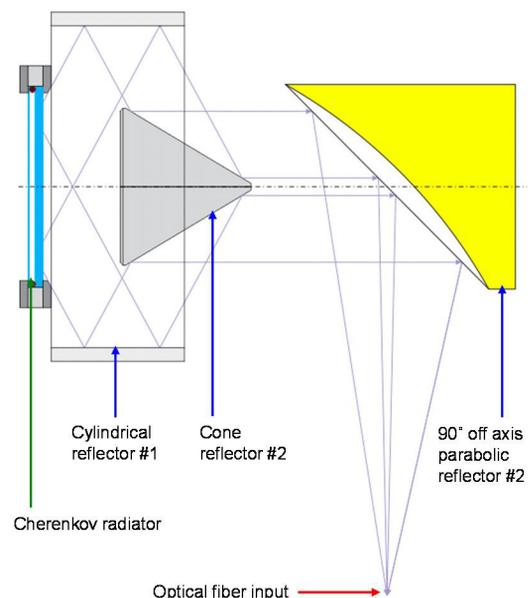

Figure 2: A loss shower emits light in a Cherenkov radiator. The light couples to an optical fibre leading to a PMT outside the tunnel. (P. Evtushenko)
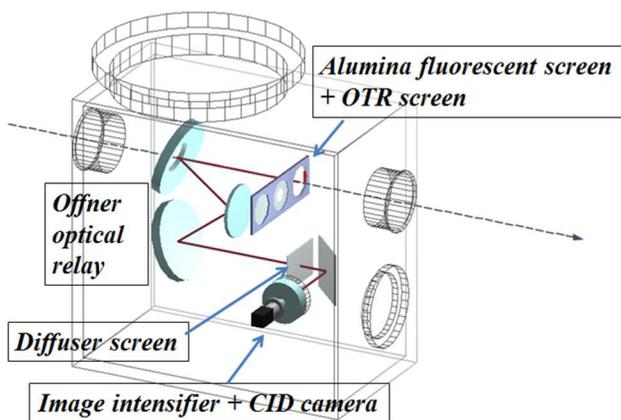
Figure 3: Two OTR screens and a fluorescent screen, with an optical relay, to image the core, tail, and halo of the J-PARC proton beam. (T. Mitsuhashi)

screens along the machine show that this tail has different Twiss parameters from those of the core.

In a wire scanner, the loss shower caused by moving a wire through a beam is detected by a scintillator or by Cherenkov radiation in a radiator or optical fibre. A photomultiplier (PMT) detects the emitted light. Since some PMTs have dark currents as low as a few nA, they can provide a high dynamic range when combined with appropriate electronics.

Pulse counting is feasible for beams with high repetition rates, such as in CEBAF. Paired measurements in coincidence can further reduce background. At lower rates, a gated analogue integrator can provide a wide dynamic range. Using two integrators with sensitivities differing by a factor of 100 can further extend the range to 10^6. Logarithmic current-to-voltage converters with a dynamic range of 10^8 to 10^{10} are being evaluated as an alternative, although the noise behaviour and bandwidth are more complex.

A Cherenkov radiator with efficient reflective optics coupling its light into a fibre was also described (Figure 2). The fibre brings the light to a PMT placed outside the tunnel to reduce background.

OTR and Fluorescent Screens

Toshiyuki Mitsuhashi (KEK) described the use of three targets to image the 3.5-GeV proton beam in J-PARC: an OTR screen to capture light from the core, an OTR with a central hole for the tail, and four fluorescent screens at large |x| and |y| to obtain more sensitivity for the halo. An OTR image using a foil at 45° to the beam would be blurred by the short depth of field resulting from the beam's wide OTR angular distribution. Instead, forward emission at normal incidence is collected by a mirror with a central hole, the first stage of an Offner optical relay (Figure 3).

The intensity scales of the three measurements can be matched over portions of the beam profile covered by two images, to get the combined horizontal profiles of Figure 4. The collimators are removed in 4a but inserted in 4b. We see the importance of making halo measurements while collimating: here its effect is to increase the halo.

Bent Crystals

Uli Wienands (SLAC) pointed out that although crystal collimation of protons has shown some promise, it has not been thought suitable for electrons due to a lower channelling efficiency and enhanced scattering. However, a recent test at SLAC (T-513) shows that a related process, volume reflection (Figure 5a), can efficiently deflect electrons (5b) in a mosaic Si crystal with a slight bend of 0.4 mrad, reducing the tail by a factor of 10.

NON-INVASIVE, NON-OPTICAL TECHNIQUES

Gas Jets

Adam Jeff (CERN and University of Liverpool) compared two ways to make an ionization profile monitor with a gas jet. In one, a thin gas sheet crosses a proton beam at angle (typically 45°). An electric field draws the ions transversely to a microchannel plate and phosphor screen. The space charge created by the sheet can distort the image. Alternatively, he proposed a thin "pencil" jet
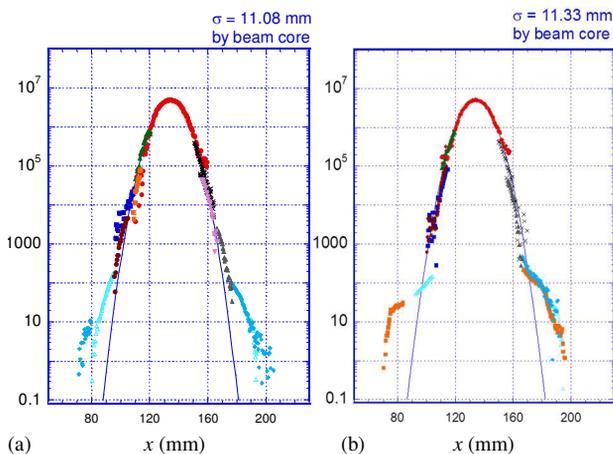

Figure 4: Horizontal profiles (log scale) of the J-PARC proton beam, combined from three types of screen; (a) without and (b) with collimation. (T. Mitsuhashi)
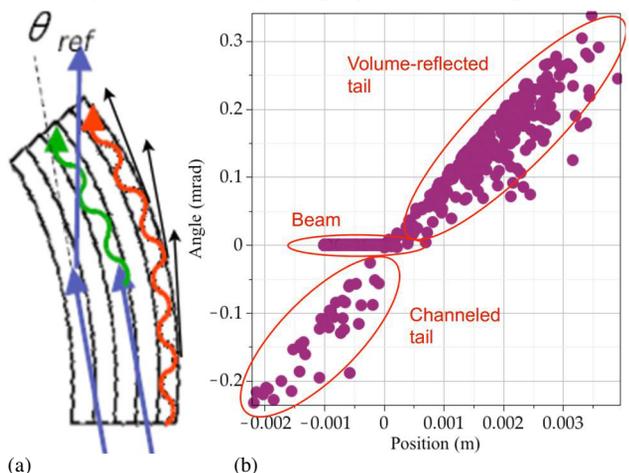

Figure 5: (a) Volume reflection (left) and channelling (centre and right) in a bent crystal. (b) Channelled and reflected electrons in T-513 at SLAC. (U. Wienands)
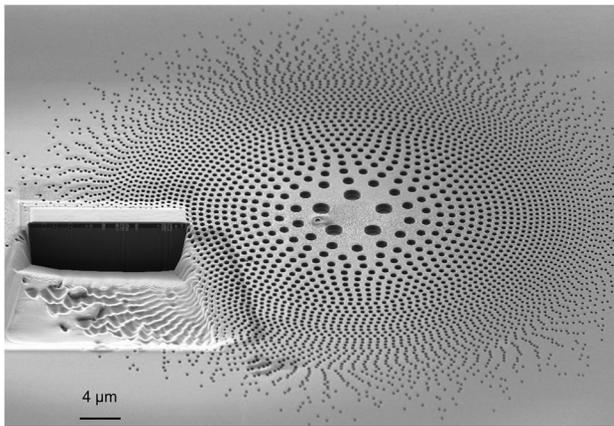
Figure 6: An atomic sieve to focus a thin gas jet. (A. Jeff)

of gas that scans across the beam, quickly though the core and slowly through the tail and halo.

Such a thin jet could be made with the matter-wave analogue of a Fresnel zone plate. This has been demonstrated [5] with room-temperature helium, which has a deBroglie wavelength of 0.05 nm. With a monoenergetic source, the focal size would be comparable to the 100-nm width of the outer zone. However, zone-pate focusing is strongly chromatic and so gave a still impressive resolution of 2 μm FWHM.

A "photon sieve" [6] for x-ray imaging replaces the rings with a pattern of holes that give a sharper focus and easier fabrication. At the time of the workshop, the corresponding structure for matter waves, an "atomic sieve" (Figure 6) for a gas jet, was being fabricated.

Beam-Gas Vertex Detector

Rhodri Jones (CERN) described beam-gas measurements of the distributions of the two proton beams near the IP of the LHCb detector. The vertex locator (VELO), a series of radial and azimuthal silicon-strip sensors, records the charged-particle tracks. Reconstructing the vertices of these events gives the proton distributions (Figure 7a), from which the luminosity overlap integral can be computed. Pulsed gas injection has been used to speed data accumulation. Beam-gas has measured the relative charges in the individual bunches, comparing well with the fast bunch-current transformer, and has measured unbunched ("ghost") charge.

A new instrument, BGV, is being developed using gas injection into a chamber with differential pumping (Figure 7b). It may have capabilities for measuring halo at 4 to 6 sigmas from the core, although the beam-gas rate will be orders of magnitude smaller. It may be possible to find the average halo in the beams. A large increase in pressure, perhaps with a gas sheet or jet, could be helpful.

Scattered Electrons

Peter Thieberger (BNL) presented a tool for co-aligning two electron lenses with the RHIC beams, with a tolerance of 30 μm. In an electron lens, the electro-magnetic field of a low-energy electron beam (~5 keV) focuses the high-energy (100 GeV/amu) protons or ions
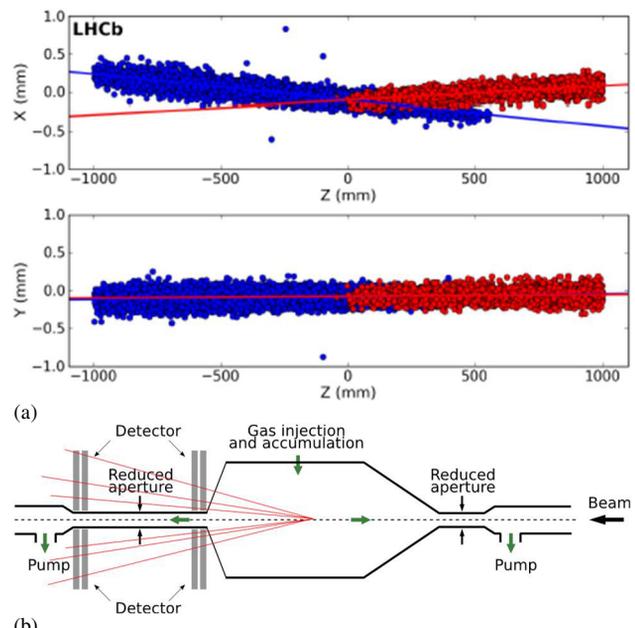

(a)

(b)

Figure 7: (a) Proton distributions in the LHC determined from beam-gas vertices. (b) A design sketch of the BGV. (R. Jones)

travelling in the opposite direction. Electrons back-scattered from the beam produce an alignment-dependent signal in a scintillator and PMT. Scattering of electrons in residual gas contributes to background and so necessitates excellent vacuum.

A hollow electron beam (a cylindrical shell) could probe beam halo by backscattering. Figure 8 shows a conceptual design.

OPTICAL TECHNIQUES

Any discussion about optical techniques for observing a dim halo in the vicinity of a bright core begins with a related problem from astronomy: viewing the solar corona. A million times dimmer than the sun's disc, the corona is normally visible only during an eclipse, when the moon blocks the sun's light. Many unsuccessful attempts were made to image the corona on a more convenient schedule by inserting a similar stop at an intermediate image plane inside a telescope. The problem was finally solved in 1934 by Bernard Lyot [7], who noted that the Airy diffraction rings from a telescope's entrance aperture or first optic overlap the image of the
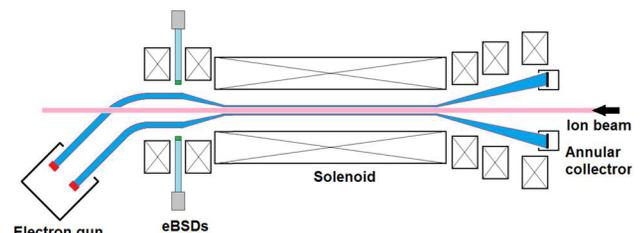

Figure 8: A hollow electron lens with electron back-scattering detectors (eBSDs) for measuring beam halo. (P. Thieberger)
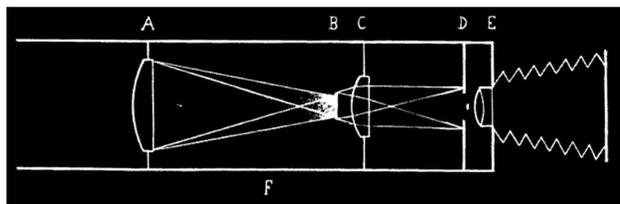
Figure 9: Lyot's coronagraph [7]. The image of the sun formed by lens A is blocked by stop B, which passes light from the corona. Lens A is imaged by lens C onto aperture D—the "Lyot stop"—but D blocks the image of A's edge, removing the Airy diffraction rings. The corona is imaged by lens E onto the film. See [8].
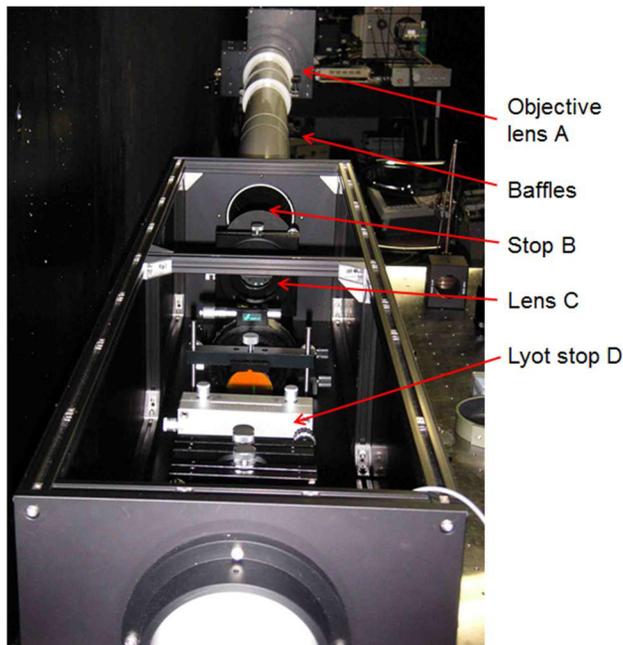

Figure 10: Coronagraph at the Photon Factory. (T. Mitsuhashi)

corona and are much brighter. He blocked them with a second stop (Figure 9). In contrast, a telescope viewing a solar eclipse is entirely within the large umbra of the moon and so can see the corona without competition from diffraction rings.

A Coronagraph for Beam Halo

Toshiyuki Mitsuhashi (KEK) explained the principle of the coronagraph and described one he built to observe beam halo in the Photon Factory (Figure 10). He emphasized design issues such as scattering from defects and dust on the surface of the objective lens or relay mirrors, and background from reflections inside the instrument. Light from the beam is split into two paths, providing simultaneous images of the core and halo (Figure 11).

Digital Micro-Mirror Arrays

Digital micro-mirror arrays (DMAs) are commonly used in computer projectors. **Jeff Corbett** (SLAC) described measurements with a DMA having a grid of 1024×768, 13.7-μm-square mirrors. When powered,
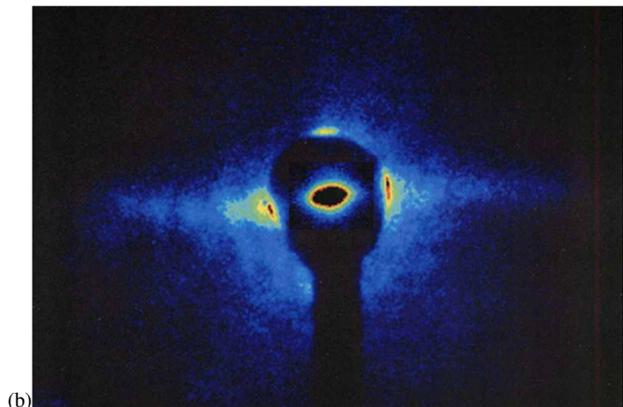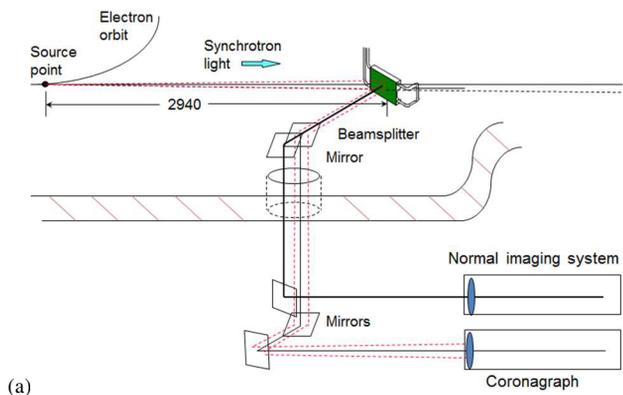

(a)

(b)

Figure 11: (a) The dual optical transport line for synchrotron light at the Photon Factory sends light to both a standard imaging system and the coronagraph. (b) Superimposed images of the beam's core and halo. (T. Mitsuhashi)

each mirror tilts to one of two positions, rotating about one diagonal by ±12° under programmed control (Figure 12). In studies on the SPEAR3 ring at SLAC, a synchrotron-light image of a beam was separated into core and halo by reflecting the light from these regions in two directions.

A fast gated camera with a Peltier-cooled detector was set for a constant 2-ms exposure. With the full DMA reflecting the light to the camera, and with a neutral-density (spectrally flat) optical filter attenuating by 10^5, the camera showed only the core. Mirror segments were then toggled to remove light from regions of the image
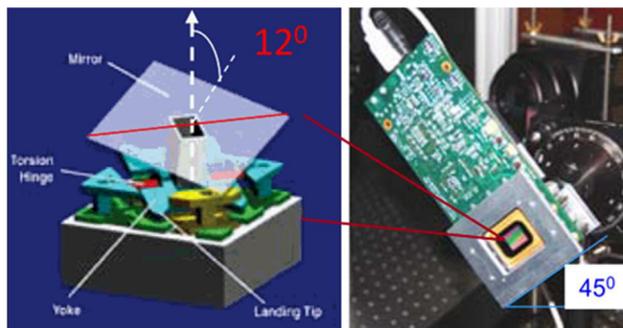

Figure 12: One micro-mirror (left) and the full DMA (right). The test board was mounted at 45° so that the two reflections remained on the horizontal plane. (J. Corbett)
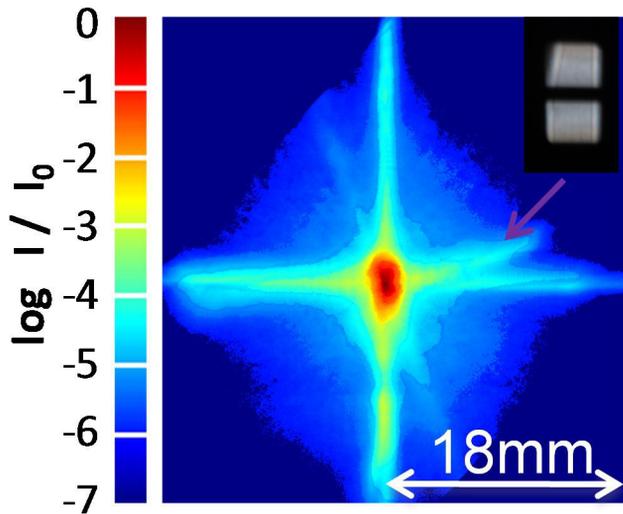
Figure 13: This composite beam image (log scale showing 7 orders of magnitude) was created in 6 steps. The brightest 90% of the previous image was removed by toggling the DMA mirrors while reducing the optical attenuation by 10. The inset shows incoming light from the transport line. The central black bar is the shadow of a cooled mask on the midplane that blocks synchrotron x rays. (J. Corbett)

with intensities greater than 10% of maximum, the optical attenuation was reduced by 10, and a new image was taken. This continued in steps of 10 until no filter was used. The brightest regions in the final image were five orders of magnitude below the peak of the core, and the dynamic range of the camera went two or more orders below this. Figure 13 shows a composite image of the intensity on a logarithmic scale.

Amplitude Apodizers

The diffraction rings removed in Lyot's coronagraph originate in the Fourier transform of the entrance aperture. Making this sharp-edged "pupil function" more gradual lessens the severity of the diffraction. Mitsuhashi addressed this briefly at the end of his coronagraph talk.
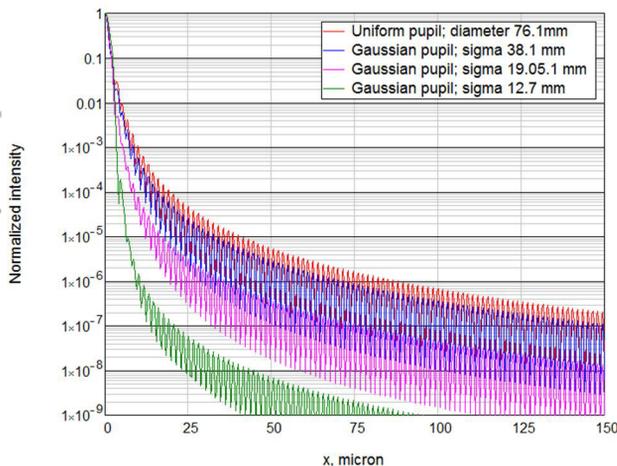

Figure 14: Point-spread functions of a hard edge and of various Gaussian apodizers. (P. Evtushenko)
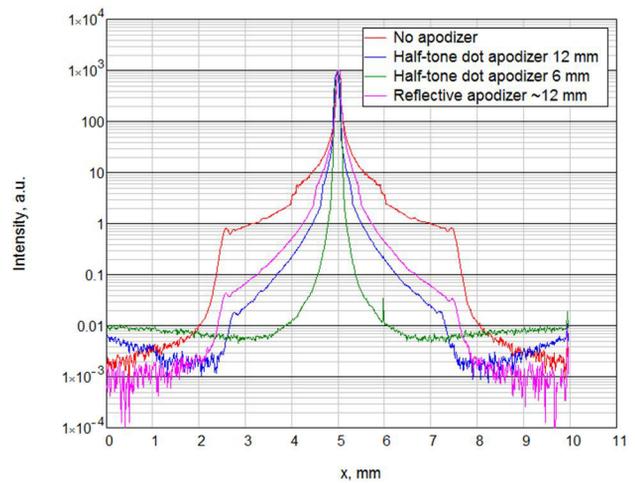
Figure 15: Line-outs (log scale) across the centre of images of a pinhole, with various apodizers at the lens. (P. Evtushenko)

Pavel Evtushenko (Jefferson Lab) returned to this theme, showing the image of a point source on the transform plane (the "point-spread function") after the aperture is replaced by Gaussian "apodizers" of various widths (Figure 14). Although narrowing an aperture generally worsens the diffractive resolution limit, the effect of softening the edge dominates in this range. A similar improvement results when these point-spread functions are convolved with a Gaussian beam.

A Gaussian transmission function can be approximated by a carefully designed pattern of black dots on a transparent base—a "half-tone dot apodizer". If the dots are small enough, their high spatial frequencies do not affect the image. In Figure 15, a pinhole source is imaged onto a CCD camera. The central line is compared for: no apodizer, a continuous reflective Gaussian apodizer, and two Gaussian dot apodizers of different widths. We see that the narrow dot apodizer has the best performance.

Astronomical Techniques

The concluding workshop talk returned fully to astronomy. **Sandrine Thomas** (NASA Ames Research Centre and University of California Santa Cruz) discussed optics descended from Lyot's that are being prepared for the direct observation of planets orbiting nearby stars. This objective, seeing a dim exoplanet close to a bright star, is comparable to observing beam halo optically, but even more demanding.

Nearly 1000 confirmed exoplanets, plus almost 3000 candidates, have been found to date, but most detection used either the dimming of the light as the planet's orbit briefly transits between the star and the Earth, or gravitational effects: the star's wobble, shifting its position and Doppler shifting its light, or gravitational microlensing as the planet changes the apparent position of a distant star in line with it. Direct detection of an Earth-like planet would enable spectroscopy of the planetary atmosphere. However, seeing the planet requires a dynamic range of 10 orders of magnitude. Thomas compared the task to

"searching for a firefly next to a lighthouse in San Francisco from Boston". Two approaches are in development: advanced coronagraphs and a "starshade".

Lyot's design can be improved with the micro-dot apodizer discussed previously, as well as with adaptive optics—deformable mirrors and wavefront sensors in feedback—to control static and dynamic aberrations. The gains can be seen in the simulations of Figures 16 to 18.

The starshade returns to the more favourable optics of a solar eclipse, by blocking the starlight with a large stop far from the telescope. An "occulter", a 32-m-diameter with a sunflower-shaped edge to approximate an apodizer, would sit at the Sun-Earth L_2 Lagrange point, 40,000 km from a space telescope, and allow the telescope to see a planetary system around a star in direct line with the starshade. The distant location of the occulter makes this scheme less suitable for viewing beam halo than the coronagraph.

CONCLUSIONS

Any device to measure beam halo is challenged by the need to span a dynamic range of 10^6 and to determine that these measurements are not influenced by background.

With careful design, two of the invasive techniques presented, the wire scanner and the combined OTR and fluorescent screens, have shown this capability, but invasive measurements are not suitable for many purposes. The other non-optical methods are at this time more speculative for halo monitoring.

Optical methods with high dynamic range have been demonstrated, including the DMA and others not presented here [9]: a charge-injection device (CID) camera and a small, masked, moving PMT. The composite image from the DMA (Figure 13) has a wide dynamic range. However, any optical method is subject to background light from sources other than halo, such as diffraction of light from the core or from the micro-mirrors themselves, scattering from imperfections in upstream optics, or reflection from the chamber walls. The DMA, CID, and scanned PMT can give a measure of the point-spread function of the optics (while folding in the bunch size), but further work is needed to determine that the halo dominates over the background.

NASA Ames has a laboratory with both the detection optics a careful simulation of the sources. Optical halo techniques should be developed in a similar setting, with light sources widely adjustable in size, position and intensity, to represent the core and halo. After an optical system is installed in a beamline, interference from wall reflections and imperfections in viewports can be probed by seeing whether any halo image is affected by moving collimators, changing background pressure, or otherwise influencing the halo distribution.

ACKNOWLEDGMENT

I thank my accelerator colleagues who stayed on after IBIC 2014 to attend the workshop and to present and discuss the work on beam-halo measurements. I also want
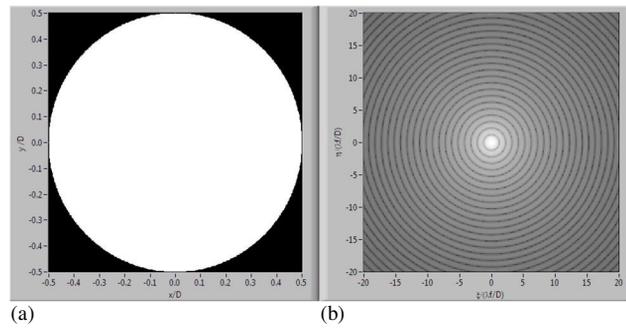

Figure 16: In this series of simulations, (a) a uniformly illuminated lens with a hard-edged entrance aperture has (b) diffraction rings one focal length away that are too bright to detect a planet. (S. Thomas)
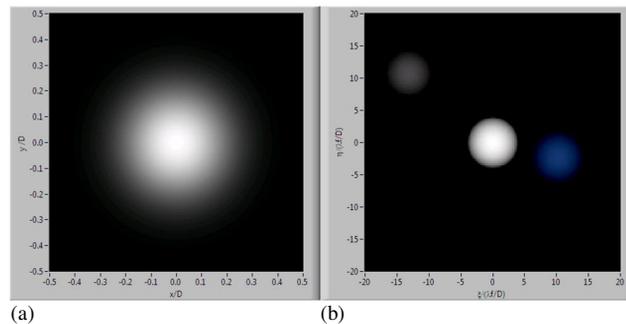

Figure 17: (a) Inserting an apodizer at the lens of Figure 16 sharpens the image, removes the rings, and brings two planets into view. (S. Thomas)

to thank Sandrine Thomas for presenting related efforts in astronomy to a meeting of accelerator physicists. She and her colleagues at NASA Ames took time to show me their lab and to discuss their approach to our common optical problems. We have much to gain from collaboration.

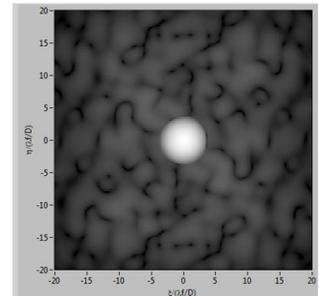I thank all the speakers for allowing SLAC to post their contributions on-line [3].

Figure 18: But if the lens has aberrations, the planets in Figure 17 cannot be seen. (S. Thomas)

REFERENCES

[1] https://portal.slac.stanford.edu/sites/conf_public/bhm_2014/Lists/registration/Public_view.aspx

[2] https://portal.slac.stanford.edu/sites/conf_public/bhm_2014/Pages/default.aspx

[3] https://portal.slac.stanford.edu/sites/conf_public/bhm_2014/Presentations/Forms/AllItems.aspx

[4] M. Yoshimoto, "Development of the Beam-Halo Monitor in the J-PARC 3-GeV RCS", Proc. IPAC 2012, WEOAA03, New Orleans, LA, USA.

[5] T. Reisinger, S. Eder, M.M. Greve, H.I. Smith, B. Holst, "Free-Standing Silicon-Nitride Zone Plates for

Neutral-Helium Microscopy", Microelectronic Engi–neering 87 (2010) 1011.

[6] L. Kipp, M. Skibowski, R.L. Johnson, R. Berndt, R. Adelung, S. Harm and R. Seemann, "Sharper Images by Focusing Soft X-Rays with Photon Sieves", Nature 414 (2001) 184.

[7] M.B. Lyot, "A Study of the Solar Corona and Prominences without Eclipses", Monthly Notices of the Royal Astronomical Society 99 (1939) 580.

[8] A. Sivaramakrishnan, C.D. Koresko, R.B. Makidon, T. Berkefeld and M.J. Kuchner, "Ground-Based Coronography with High-Order Adaptive Optics", Astrophys. J. 552 (2001) 397.

[9] C.P. Welsch, E. Bravin, B. Burel, T. Lefèvre, T. Chapman and M.J. Pilon, "Alternative Techniques for Beam Halo Measurements", Meas. Sci. Technol. 17 (2006) 2035.